Entrainment to extinction of physiological tremor by spindle afferent input

Ian Cathers*, Nicholas O'Dwyer+, Peter Neilson#

Schools of Biomedical Sciences* and Exercise and Sport Science+, The University of Sydney, Australia

Neuroengineering Laboratory, School of Electrical Engineering and Telecommunications, University of New South Wales, Sydney, Australia

Address for Correspondence: Ian Cathers
School of Biomedical Sciences
Faculty of Health Sciences
The University of Sydney
PO Box 170
Lidcombe, NSW 1825
Australia

email: i.cathers@fhs.usyd.edu.au
Phone: (+61 2) 9351 9287
Fax: (+61 2) 9351 9520

Abstract

In this study the systematic modulation of wrist flexor muscle activity by imposed joint movement was examined. Ten subjects maintained a constant contraction level (25% of maximum; trial duration: 20 s) in flexor carpi radialis while their wrists were perturbed with 50 different quasi-sinusoidal signals (frequency range: 0.5 - 9.5 Hz; amplitude: 0.3° - 4.2°). Frequency spectra of wrist position and the rectified and filtered electromyogram (EMG) were determined. The muscle activity was only weakly entrained to imposed movements of small amplitude and low frequency, as shown by a small peak in the EMG spectrum at the frequency of movement, while the most prominent peak in the spectrum was between 9 - 15 Hz, corresponding to the frequency range of physiological tremor. The entrainment of muscle activity increased markedly as the amplitude and frequency of the imposed movement increased, to the point of saturation of modulation and harmonic peaks in the spectrum. In parallel with this increase in entrainment, the 9 - 15 Hz tremor peak was progressively extinguished. The results are consistent with a coupled oscillator model in which the central oscillatory source(s) of tremor became fully entrained to the imposed movement at the highest amplitudes and frequencies. Such coupling depends on communication between the external forcing oscillator and the central oscillator(s), the Ia afferent signal from the imposed movement being the most likely candidate to provide the entraining signal for the central oscillator(s).

Key Words: stretch reflex, tremor, coupled oscillators, neural modeling, wrist, electromyography

Introduction

Physiological or *normal* tremor at the wrist is an involuntary rhythmical movement typically in the frequency range of 8 - 12 Hz and is usually of such small amplitude that it cannot be seen with the naked eye. A number of sources of physiological tremor have been suggested, including mechanical resonance of the limb (Joyce and Rack 1974; Elble and Randall 1976, 1978; Brown et al. 1982a; Burne et al. 1984), synchronisation of motor unit firing (Elble and Randall 1976; Allum et al. 1978; Marsden 1984; Elble and Koller 1990; Matthews 1997; Timmer et al. 1998a,b; see also Halliday et al. 1999) and instability within the stretch reflex arc (Lippold 1970, 1971; Young and Hagbarth 1980; Zahalak and Cannon 1983; Burne et al. 1984; Young 1984, Graham and Redman 1993; Miao and Sakamoto 1997; Sakamoto et al. 1998; Santillan et al. 2003). The multifactorial nature of tremor was emphasised by Llinas who described it as an "emerging property of various components" (Llinas 1984, p.178).

Since a limb acts as an underdamped second order mechanical system, it has a tendency to oscillate at its natural frequency. However, when the frequency of the mechanical component of physiological tremor is reduced by increasing the mass loading of the limb (Joyce and Rack 1974; Brown et al. 1982a), a component at 8 - 12 Hz remains constant or even shifts to slightly higher frequencies (Elble and Randall 1976; Elble and Randall 1978), suggesting that it has a neural origin. There is a tendency for unfused or partially fused motor unit twitches to cause tremor and while the mean motor unit firing frequency is somewhat higher than the frequency of physiological tremor, there is a tendency for short-term clustering of firing in the range of 8 - 12 Hz (Elble and Randall 1976; Elble and Koller 1990; see also Halliday et al. 1999). The underdamped

oscillations of physiological tremor have also been associated with oscillations in the stretch reflex arc (Lippold 1970, 1971) and tremor may be enhanced by manipulations which increase the gain around the reflex arc (Young and Hagbarth 1980; Young 1984) or attenuated via limb restriction (Burne et al. 1984). Some models of the stretch reflex have shown oscillations similar to observed tremor (Zahalak and Cannon 1983; Graham and Redman 1993; Miao and Sakamoto 1997; Sakamoto et al. 1998; Santillan et al. 2003).

Since the stretch reflex as well as neural and mechanical oscillators contribute to the generation of physiological tremor, it would be expected that an oscillatory stimulus that elicits a stretch reflex would interact with the neural and mechanical oscillators. Thus, entrainment of both parkinsonian (Rack and Ross 1986) and essential (Elble et al. 1992) tremor by the stretch reflex has been reported. In normal subjects, prominent 8-12 Hz physiological tremor is commonly detectable in the electromyogram (EMG) despite little discernible wrist tremor (Elble et al. 1987). In the present investigation it is shown that these EMG oscillations from physiological tremor can be strongly entrained by a stretch stimulus. The degree of entrainment was dependent of the amplitude and frequency of stretch, such that tremor EMG disappeared completely as the amplitude of stretch increased and the frequency of stretch approached the tremor frequency. A simple model of the stretch reflex, consisting of a spindle input to an integrate and fire motor neuron, replicated the entrainment found experimentally. The study is the first systematic investigation of a frequency- and amplitude-dependent saturation of modulation of the stretch reflex response in humans.

Materials and Methods

The data for this study are a subset of those from a previous study of the amplitude and frequency dependence of the stretch reflex (Cathers et al. 1999). Different analytical tools have been used here to elucidate interactions between physiological tremor and the stretch reflex. The experimental arrangements and procedures are reviewed below and the signal analysis is described in detail.

Subjects

Ten subjects (6 male and 4 female), ranging in age from 31 to 46 years (mean=39, SD=4.9) and with no previous history of musculoskeletal or neurological disease participated in these procedures. The right arm was tested and was the dominant arm for all subjects. The experimental procedures were approved by the University of Sydney Human Ethics Committee and subjects gave their written informed consent prior to testing.

Equipment

Subjects were seated with the shoulder abducted at approximately 45^{o} and elbow flexed at approximately 100^{o}. The forearm was firmly strapped into a support which allowed rotation of the wrist. The hand grasped a vertically oriented 43 mm diameter handle of a manipulandum. By adjusting the position of the handle, the wrist was located directly above the rotational axis of the manipulandum.

The manipulandum was fixed to the shaft of a DC motor providing a peak torque of 16 Nm. The motor was configured as a position control servo with the reference signal being provided from a computer-driven digital to analog card and position feedback from a rotary induction transducer fixed to the shaft of the servo motor. Wrist angle was also monitored via this transducer. The stiffness of the servo was such that repeated trials using the same input signals produced highly reproducible (within 5%) wrist displacements within and between subjects.

Two silver/silver chloride surface electrodes of 10 mm diameter were fitted with centres 25 mm apart, 90 mm distal to the medial epicondyle of the humerus and approximately 15 mm medial from the mid-line of the forearm. This positioning of the electrodes allowed maximal pick-up of signals from the flexor carpi radialis muscle (Delagi et al. 1975). The EMG signal was amplified (gain = 1 000, bandwidth = 50 Hz - 1 kHz) and monitored on a computer display. The EMG signal was also rectified and low-pass filtered with a time constant of 0.5 s and displayed to the subject on a computer monitor to provide feedback of average contraction level. The raw EMG and the angle signals were digitised at a rate of 2 kHz and stored on computer disk for later analysis.

Displacement Signals

Fifty displacement signals were investigated, comprising 10 different frequencies and five different amplitudes. The signals had bandwidths of approximately 1 Hz, centred at 10 frequencies from 0.5 Hz to 9.5 Hz in 1 Hz steps. Each was generated using a sinusoidal function with a varying phase, which produced a signal having a nearly constant amplitude but a frequency that varied over a narrow range. Each one of these

10 frequency signals was then scaled to five different amplitudes spanning a physiologically relevant range, specified as mean rectified wrist displacements of 0.3^{o}, 0.7^{o}, 1.3^{o}, 1.9^{o} and 4.2^{o}. A three-second sample of the signal having a centre frequency of 4.5 Hz and a mean displacement of 1.3^{o}, is shown together with its power spectrum in Figure 1.

Procedures

Subjects were instructed to flex the wrist against the handle while maintaining a contraction level of 25% of maximum, using the computer monitor display of the rectified and filtered EMG activity. This contraction level was chosen because it results in coherent reflex responses (Cathers et al, 2004) while still minimising fatigue during each trial. The duration of each trial was 20 seconds. The presentation order of the 50 stimulus signals (5 amplitudes x 10 frequencies) was randomised within and across subjects. At least one minute rest was given between each stimulus presentation and no experimental session took longer than 2 hours.

Signal Analysis

The digitised EMG signals were first full-wave rectified. The angle and rectified EMG signals were then low pass filtered at 45 Hz (6^{th} order Butterworth).. These rectified and low pass filtered EMG signals will henceforth be referred to as IEMG. The data were then resampled at 100 Hz. The Fourier transform of the autocorrelation function was then computed to provide the power spectrum of the signals. The use of a sampling rate of 100 Hz together with 100 lags in the autocorrelation function resulted in a frequency resolution in the analysis of 0.5 Hz up to 50 Hz.

The overall coherence (also called “weighted coherence”; see Porges et al 1980) between wrist angle and IEMG was calculated. This provides a measure of the fraction of the total IEMG variance (power) that is accounted for by the linear relation with the angle signal. Overall coherence is based on the total power across all frequencies in the spectrum, in contrast to the typical use of coherence which is based on the power at individual frequencies. The measure may take a value in the range of 0 to 1, where 0 indicates that there is no linear relationship between the signals, while 1 signifies that there is a perfect linear relationship. In this context, a low value of overall coherence indicates weak entrainment of the reflex to stretch, whereas a high value indicates that the muscle activity is highly entrained to stretch. This is illustrated by the samples of wrist angle and IEMG data in Figure 2. The muscle activity in Figure 2a is only weakly entrained to stretch, with an overall coherence between angle and IEMG of 0.02, while the muscle activity in Figure 2b is highly entrained to stretch, as borne out by an overall coherence value of 0.41.

Repeated measures analyses of variance (ANOVAs) were carried out to determine the statistical significance of the experimental effects observed. The factors in these analyses were the amplitude and frequency of the muscle stretch stimuli. Statistical significance was accepted at probabilities less than 0.05.

Results

The major findings of the study are contained in the group mean spectra of the IEMG responses to each of the 50 stimulus signals in Figure 3. Each row shows the spectra for the five amplitudes at each frequency of stretch, while each column shows the spectra for 10 frequencies at each amplitude of stretch. A number of steps were taken in order

to maximise the visibility of smaller peaks in these spectra. First, amplitude rather than power spectra were computed because smaller peaks can be seen more clearly in such spectra. Second, for each subject, the spectrum for each stimulus signal was normalised to the subject's maximal amplitude across the 50 stimulus signals. The mean spectrum across subjects was then calculated for each stimulus signal. Finally, each mean spectrum was scaled maximally for display purposes. Three important features summarise the pattern in these spectra.

1) *Stretch stimulus frequency*

There was a peak in each spectrum at the muscle stretch frequency (the dashed line in each column passes through the 10 stretch frequencies). The size of the peak at the stretch frequency increased with amplitude of stretch (left to right across the rows) and with frequency of stretch (down the columns). This reflects the well-established fact that the amplitude of the reflex increases with both amplitude and frequency of stretch.

2) *Tremor at smaller amplitude and lower frequency of stretch*

For stretches of smaller amplitude and lower frequency (top left quadrant of Figure 3), the spectra had a peak in the tremor frequency range of 9 - 15 Hz. Although variable in exact frequency, this peak was clearly present in the spectra for eight of the 10 subjects and was substantially broader than the stretch stimulus peaks. The tremor peak decreased with increasing amplitude and frequency of stretch (left to right across the rows and down the columns) and was not present at all in the highest amplitude-frequency combinations (bottom right quadrant of Figure 3).

3) *Harmonics at larger amplitude and higher frequency of stretch*

For stretches of larger amplitude and higher frequency, there were peaks in the IEMG spectra at harmonics of the stretching frequency (eg, 8.5, 17, 25.5, 34 Hz). A numerical examination of the spectra revealed even a 6^{th} harmonic in one subject. The harmonic peaks became less evident with decreasing amplitude and frequency of stretch (right to left across the rows and up the columns) and were not present at all in the lower amplitude-frequency combinations (top left quadrant of Figure 3).

It can be seen from these three features that the frequency distribution of the IEMG activity changed systematically with the amplitude and frequency of stretch. As the size of the peak at the stretch frequency increased, the peaks at harmonics of the stretching frequency became more evident, while the peak in the tremor frequency range gradually decreased and disappeared. At intermediate amplitude-frequency combinations (eg, 1.3° - 5.5 Hz), harmonic peaks were present on tremor peaks, but either tremor peaks or harmonic peaks alone were present at either end of the amplitude-frequency range. Hence, there was a complementary relation between the stretch and harmonic peaks on the one hand and the tremor peaks on the other.

Quantification of this mutually exclusive pattern was undertaken by partitioning the frequency power spectrum of the IEMG activity up to 25 Hz into two bands: a narrow band centred on the stretching frequency (*stretch* band) and a band from 10.5 - 15 Hz centred on the tremor frequency (*tremor* band). The frequency window used to determine the *stretch* band was 2 Hz centred on the stretching frequency (for the 0.5 Hz stretch stimulus, the window could only be 1.5 Hz wide i.e. 0 - 1.5 Hz). The frequency bands for *tremor* and *stretch* were chosen so as to overlap as little as possible at the

higher frequencies of stretch, but some overlap was unavoidable and some of the harmonics of stretches at 5.5 Hz, 6.5 Hz and 7.5 Hz were included in the 10.5 - 15 Hz band. Furthermore, in order not to overlap with the 9.5 Hz stretch peaks, frequencies from 9 - 10.5 Hz were not included in the *tremor* band. The power in the stretch and tremor bands was normalised by expressing it as a fraction of the total power in the spectrum for each subject in each trial.

The mean distribution of the *stretch* and *tremor* band power across subjects is shown in Figure 4 for the five amplitudes and 10 frequencies of stretch. As the amplitude of stretch increased (across the panels), the proportion of power in the *tremor* band decreased and the proportion in the *stretch* band increased ($F_{(4,36)}$=10.75; P<0.001). Similarly, as the frequency of stretch increased (within the panels), the proportion of power in the *tremor* band decreased and the proportion in the *stretch* band increased ($F_{(9,81)}$=44.70; P<0.001). This complementary re-distribution of power could be seen even in the unscaled IEMG power spectra for individual subjects, as illustrated in Figure 5. All spectra here are shown on the same scale of absolute EMG power, in contrast with the normalised and scaled spectra in Figure 3. For stretching of 0.3^{o} at 0.5 Hz, most of the IEMG power was concentrated in the *tremor* band. At the other extreme, for stretching of 4.2^{o} at 9.5 Hz, most of the IEMG power was concentrated in the *stretch* band (and the small 19 Hz harmonic), with ostensibly no power in the *tremor* band. Between these extremes, such as a stretch of 1.3^{o} at 5.5 Hz, the power was more evenly distributed between the *stretch* and *tremor* bands.

These findings based on the frequency spectrum of the IEMG document how the muscle activity changed markedly in character as it became more strongly entrained to stretch

of higher amplitude and frequency. An appreciation of the functional significance of this effect can be gained from the raw data illustrated in Figure 2. Quantification of the effect was provided directly by the overall coherence between the signals (Figure 6). It was clear that the overall coherence rose with both increasing amplitude ($F_{(4,36)}$=45.38; P<0.001) and frequency ($F_{(9,81)}$=92.92; P<0.001) of stretch. At the lowest amplitude and frequency studied, the entrainment of the muscle to stretch accounted for only 13% of the variance of the recorded IEMG activity, whereas at the highest amplitude and frequency studied, the entrainment to stretch accounted for 62% of the variance of the IEMG activity.

Modeling of reflex behaviour

It is likely that the greater entrainment of IEMG power with increasing frequency and amplitude of stretch primarily reflects spindle and motor neuronal behaviour. A simplified model of an open-loop stretch reflex was developed using Simulink (The Mathworks) to test this proposal. The front end of this model consisted of a spindle model developed by Chen and Poppele (1978) which displays dynamics typical of other spindle models reported in the literature (for review, see Prochazka and Gorassini 1998). Of particular importance for the reflex behaviour observed in the present study is the increase in gain and phase advance of the spindle output over the frequency range tested. The output from this spindle model was connected to a simple integrate-and-fire neuron model. (Similar overall model behaviour was observed with a leaky integrator neuron model).

Figure 7a shows the neuronal output spikes of this model when there was no input to the spindle. The neuron produced a constant background firing rate of 12 Hz, which was determined by a constant input to the model neuron. Figure 7b shows how the pattern of spikes changed when a sinusoidal input to the spindle was added to the constant input. The sinusoidal input had a frequency of 1 Hz and a relative amplitude of unity. The mean frequency of the output spikes remained the same as the 12 Hz carrier produced in the absence of spindle output. However, the instantaneous spike rate was modulated by the sinusoid, resulting in a higher rate on the rising phase of the input and a lower rate on the falling phase. (Note also the phase advance of the response ahead of stretch). Figure 7c shows the effect of tripling the relative amplitude of the sinusoid. The resulting modulation of the neuron spikes was more pronounced leading to periods of quiescence during the falling phase of the input. A similar effect on the model output was produced by increasing the frequency from 1 Hz to 5 Hz (Figure 7d). The spikes were clearly locked to the rising phase of the sinusoidal inputs. An integrate-and-fire neuron model alone, without the spindle component, produced similar modulation of firing rate with changes in input amplitude, but no change in modulation with changes in input frequency.

These modeling results show that the sensitivity of reflex modulation to frequency and amplitude of stretch is the result of the integrate and fire behaviour of the neuron coupled with the encoding of the stretch signal by the spindle. Larger amplitude sinusoidal inputs result in highly entrained neuron spikes with quiescence for part of each cycle. This saturation in the encoding of the input signal results in a non-linearity in the neuron output. The saturating non-linearity which occurs with higher frequency inputs is the result of the gain characteristic of the muscle spindle, which rises

exponentially with frequency. Thus, the spindle translates high frequency inputs into large amplitude afferent signals which then drive the neuron into saturation of its modulation.

Discussion

This study has demonstrated the systematic interaction between imposed joint movement and wrist flexor muscle activity. With increases in amplitude or frequency, the imposed movement progressively took control of the afferent input and markedly increased the entrainment of the muscle activity via the stretch reflex. During small or low frequency imposed movements, the muscle activity was only weakly entrained at the frequency of stretch (overall coherence ≅ 0.1) and physiological tremor at 9-15 Hz was the most prominent peak in the EMG spectrum. During large amplitude, high frequency imposed movements, the muscle activity was powerfully entrained at the frequency of stretch (overall coherence ≅ 0.6), to the point of saturation and harmonics, in parallel with annihilation of the tremor. The saturation of the motor neuron modulation occurred at higher frequencies because the gain of the EMG reflex response increases as a power function (exponent > 1) of frequency (Cathers et al. 1999) to about 10 Hz (Neilson 1972a,b; Neilson and Neilson 1978; Zahalak and Heyman 1979; Cannon and Zahalak 1981, 1993; Cathers et al. 1999). Beyond 10 Hz, the reflex gain decreases and this may be the result of saturation (Brown et al. 1982b; Matthews 1993). The connection between saturation and input amplitude was not as strong because the

gain of the reflex decreases with amplitude (Cathers et al. 1999) and this partially offsets an increase in the amplitude of the input.

While the progressive increase in entrainment of muscle activity at the frequency of the imposed movement is readily explained by the known properties of the stretch reflex, the process of extinction of activity at the physiological tremor frequency has not been described previously. Mechanical resonance of the limb was unlikely to have played a role in this tremor EMG activity. No tremor peaks were present in the spectra of wrist displacement, due to the fact that wrist position was set by the position servo. Further, the low tendon and muscle compliance at the 25% of maximum contraction level studied would make it unlikely that there were oscillations of any significance within the muscle that were not reflected in joint movements. Therefore, while it remains possible that the 9-15 Hz physiological tremor in the EMG may derive from stretch reflex action, we would argue from the above that it must have been principally central in origin. This simplifies the situation in considering the tremor mechanisms that were operative here and appears to leave two possible explanations of the entrainment to extinction observed.

The simplest explanation is that the central and afferent sources of oscillation competed for the motor neurons, but the locus of their interaction was confined to the spinal level. The spindle input progressively took control of the motor neurons, to the point of saturation during imposed movement of large amplitude and high frequency, so that they ceased to respond to descending input from the central oscillator(s). This view is supported by the fact that the spindle and neuron model simulations reproduced the entrainment and saturation observed experimentally. This model did not incorporate a

central oscillator. It comprised only a constant drive to the neuron and spindle afferent input only onto the neuron, so the locus of the interaction between peripheral and central sources of excitation was confined to the neuron.

Although saturation of motor neuron modulation by afferent input from the imposed movement was observed, descending inputs could still modulate the motor neuron pool because, for example, subjects can readily increase or decrease the muscle contraction level under these conditions. This shows that the motor neurons had not ceased to respond to descending input and suggests that the saturation may have been confined to afferent input from the imposed movement. Therefore, a more plausible explanation for the observed entrainment to extinction of tremor activity is that the central oscillator(s) had become fully coupled to the imposed movement at the highest amplitudes and frequencies. This is a coupled oscillator model as suggested by Elble et al (1987). Such coupling depends on communication between the oscillators, the most likely candidate being the Ia afferent signal (Goodwin et al. 1975; Hagbarth and Young 1979; Matthews 1993; Matthews 1994) from the imposed movement (the external forcing oscillator) providing an entraining signal for the endogenous rhythm of the motor neurons (the central oscillator). Obviously, the communication operated only in one direction here, from the forcing oscillator to the central oscillator. In the absence of this communication, the oscillators would not have interfered with each other but instead would have continued to operate independently, so that the magnitude of the central oscillator (tremor) would not have altered as the magnitude of the forcing oscillator (stretch) increased. In accordance with basic oscillator theory, the tremor was more powerfully entrained the closer the relative frequencies of the two oscillations (cf, 9.5 Hz movement in Figure 3) and the larger the relative amplitude of the external forcing

oscillator. Indeed, it is notable that even at the most distant relative frequencies, the tremor was significantly entrained by the largest amplitude of the forcing oscillator, as shown by an overall coherence of 0.12 (cf, 0.5 Hz movement in Figure 3). Furthermore, only the central source(s) of oscillation apparently became coupled to the imposed movement and other sources of descending input, such as voluntary drive, were not affected.

It has been shown previously that it is possible to entrain both essential (Elble et al. 1992) and parkinsonian (Rack and Ross 1986) tremor to imposed movement. However, these pathological tremors often precluded entrainment to the imposed movement and entrainment only occurred when the forcing oscillator was large in amplitude and close to the frequency of the tremor. This is consistent with the progression of entrainment observed here, but the entrainment here occurred far more readily, over a broader range of amplitudes and frequencies, than in both cases of pathological tremor. This suggests 1) that the central oscillatory mechanism(s) of normal physiological tremor are far more responsive to communication from afferent input or 2) that the central oscillator(s) of physiological tremor compete far less strongly for motor neurons than is the case with the oscillatory mechanisms responsible for these pathological tremors.

The presence in the EMG signal of harmonics of the stretching frequency which do not correspond to any power in the stretching stimulus (Figures 3 and 5) is an important non-linearity (eg, see Winter and Patla 1997). One possible cause of this would be multiple EMG bursting on each stretch cycle, as has been reported previously (Andrews et al. 1973b; Rack et al. 1983), but examination of the raw data provided no evidence for multiple bursting here. The raw data in Figure 2b show a case where harmonics

were strongly present, taken from the subject whose spectra are shown in Figure 5, at an amplitude of 1.9^{o} and frequency of 8.5 Hz. Despite the fact that the subject maintained a constant average contraction level of 25% of maximum, the EMG modulation was so deep that the signal 'bottomed out' at zero between bursts and so the EMG modulation departed significantly from the quasi-sinusoidal waveform of the movement input. When this type of EMG signal is rectified and low-pass filtered, it exhibits truncation in which the negative-going segments of the waveform become flattened. Spectral decomposition of such a truncated waveform results in harmonics. Examination of the raw data confirmed that this pattern was seen in all cases where harmonics of the stretching frequency were present. Studies in the cat have shown similar discrete bursts of activity phase-locked to cyclic stretching which became more probable as the amplitude of the stretch increased (Jansen and Rack 1966; Rosenthal et al. 1970) and human studies also have shown EMG traces in which such saturation was apparent (e.g. Brown et al. 1982b). Brown et al. commented on the EMG being "well modulated by movement" (p. 95) in the 5 – 15 Hz range. This depth of modulation may be compared with that from the same subject at the same amplitude, but at a frequency of only 0.5 Hz (Figure 2a). Under these conditions, the modulation by the muscle stretch was only just apparent and there were no harmonics in the spectrum (see Figure 5). It can be seen therefore that the presence in the EMG signal of harmonics of the frequency of the imposed movement is directly related to the saturation of motor neuron modulation.

References

Allum JH, Dietz V, Freund HJ (1978) Neuronal mechanisms underlying physiological tremor. J Neurophysiol 41: 557-571

Andrews CJ, Burke D, Lance JW (1973a) The comparison of tremors in normal, parkinsonian and athetotic man. J Neurol Sci 19: 53-61

Andrews CJ, Neilson PD, Lance JW (1973b) Comparison of stretch reflexes and shortening reactions in activated normal subjects with those in Parkinson's disease. J Neurol Neurosur Ps 36: 329-333

Brown TIH, Rack PMH, Ross HF (1982a) Different types of tremor in the human thumb. J Physiol 332: 113-123

Brown TIH, Rack PMH, Ross HF (1982b) Electromyographic responses to imposed sinusoidal movement of the human thumb. J Physiol 332: 87-99

Burne JA, Lippold OCJ, Pryor M (1984) Proprioceptors and normal tremor. J Physiol 348: 559-572

Cannon SC, Zahalak GI (1981) Reflex feedback in small perturbations of a limb. ASME Biomechanics Symposium AMD(43): 117-120

Cathers I, O'Dwyer N, Neilson P (1999) Dependence of stretch reflexes on amplitude and bandwidth of stretch in human wrist muscle. Exp Brain Res 129: 278–287

Cathers I, O'Dwyer N, Neilson P (2004) Variation of magnitude and timing of wrist flexor stretch reflex across the full range of voluntary activation. Exp Brain Res 157:324-335

Chen WJ, Poppele RE (1978) Small-signal analysis of response of mammalian muscle spindles with fusimotor stimulation and a comparison with large-signal properties. J Neurophysiol 41: 15-27

Delagi EF, Perotto A, Iazzetti J, Morrison D (1975) Anatomic guide for the electromyographer. Charles C Thomas, Springfield, Il

Elble RJ (1986) Physiologic and essential tremor. Neurology 36: 225-231

Elble RJ, Higgins C, Hughes L (1992) Phase resetting and frequency entrainment of essential tremor. Exp Neurol 116: 355-361

Elble RJ, Higgins C, Moody CJ (1987) Stretch reflex oscillations and essential tremor. J Neurol Neurosur Ps 50: 691-698

Elble RJ, Koller WC (1990) Tremor. The Johns Hopkins University Press, Baltimore, MD

Elble RJ, Randall JE (1976) Motor-unit activity responsible for 8- to 12-Hz component of human physiological tremor. J Neurophysiol 39: 370-383

Elble RJ, Randall JE (1978) Mechanistic components of normal hand tremor. Electroen Clin Neuro 44: 72-82

Goodwin GM, Hulliger M, Matthews PBC (1975) The effects of fusimotor stimulation during small amplitude stretching on the frequency response of the primary ending of the mammalian muscle spindle. J Physiol 253: 175-206

Graham BP, Redman SJ (1993) Dynamic behaviour of a model of the muscle stretch reflex. Neural Networks 6: 947-962

Hagbarth KE, Young RR (1979) Participation of the stretch reflex in human physiological tremor. Brain 102: 509-526

Halliday DM, Conway BA, Farmer SF, Rosenberg JR (1999) Load-independent contributions from motor-unit synchronization to human physiological tremor. J Neurophysiol 82: 664-675

Jansen JKS, Rack PMH (1966) The reflex response to sinusoidal stretching of the soleus in the decerebrate cat. J Physiol 183: 15-36

Joyce GC, Rack PMH (1974) The effects of load and force on tremor at the normal human elbow joint. J Physiol 240: 375-396

Lance JW (1968) Physiological tremor. Lancet 1: 94

Lippold OC (1970) Oscillation in the stretch reflex arc and the origin of the rhythmical, 8-12 c-s component of physiological tremor. J Physiol 206: 359-382

Lippold OC (1971) Physiological tremor. Sci Am 224: 65-73

Llinas RR (1984) Rebound excitation as the physiological basis for tremor: a biophysical study of the oscillatory properties of mammalian central neurones *in vitro*.

In: Findley LJ, Capildeo R (eds) Movement disorders: Tremor. Macmillan, London, pp 165-182

Marsden CD (1984) Origins of normal and pathological tremor. In: Findley LJ, Capildeo R (eds) Movement disorders: Tremor. Macmillan, London, pp 37-84

Matthews PBC (1993) Interaction between short- and long-latency components of the human stretch reflex during sinusoidal stretching. J Physiol 462: 503-527

Matthews PBC (1994) The simple frequency response of human stretch reflexes in which either short- or long-latency components predominate. J Physiol 481: 777-798

Matthews PBC (1997) Spindle and motoneuronal contributions to the phase advance of the human stretch reflex and the reduction of tremor. J Physiol 498: 249-275

Miao T, Sakamoto K (1997) An investigation of stretch reflex in physiological tremor. Electromyogr Clin Neurophysiol 37: 343-357

Neilson PD (1972a) Interaction between voluntary contraction and tonic stretch reflex transmission in normal and spastic patients. J Neurol Neurosur Ps 35: 853-860

Neilson PD (1972b) Voluntary and reflex control of the biceps brachii muscle in spastic-athetotic patients. J Neurol Neurosur Ps 35: 589-598

Neilson PD (1993) Tonic stretch reflex in normal subjects and in cerebral palsy. In: Gandevia S, Burke D, M. A (eds) Science and practice in clinical neurology. Cambridge University Press, Sydney

Neilson PD, Neilson MD (1978) The role of action reflexes in the damping of mechanical oscillations. Brain Res 142: 439-453

Porges SW, Bohrer RE, Cheung MN, Drasgow F, McCabe PM, Keren G (1980) New time-series statistic for detecting rhythmic co-occurrence in the frequency domain: The weighted coherence and its application to psychophysiological research. Psychol Bull 88: 580-587

Prochazka A, Gorassini M (1998) Models of ensemble firing of muscle spindle afferents recorded during normal locomotion in cats. J Physiol 507: 277-291

Rack PMH, Ross HF (1986) The role of reflexes in the resting tremor of Parkinson's disease. Brain 109: 115-141

Rack PMH, Ross HF, Thilmann AF, Walters DK (1983) Reflex responses at the human ankle: the importance of tendon compliance. J Physiol 344: 503-524

Rosenthal NP, McKean WJ, Terzuolo CA (1970) Frequency analysis of stretch reflex and its main subsystems in triceps surae muscles of the cat. J Neurophysiol 28: 713-749

Sakamoto K, Miao T, Arihara M (1998) Analysis of interaction of spinal and supraspinal reflex pathways involved in physiological tremor. Electromyogr Clin Neurophysiol 38: 103-113

Santillan M, Hernandez-Perez R, Delgado-Lezama R (2003) A numeric study of the noise-induced tremor in a mathematical model of the stretch reflex. J Theor Biol 222: 99-115

Stein RB, Lee RG (1981) Tremor and clonus. In: Geiger SR (ed) Handbook of Physiology: The Nervous System, vol II, Motor Control, Part 1. American Physiological Society, Bethesda, pp 325-343

Timmer J, Lauk M, Pfleger W, Deuschl G (1998a) Cross-spectral analysis of physiological tremor and muscle activity. I. Theory and application to unsynchronized electromyogram. Biol Cybern 78: 349-357

Timmer J, Lauk M, Pfleger W, Deuschl G (1998b) Cross-spectral analysis of physiological tremor and muscle activity. II. Application to synchronized electromyogram. Biol Cybern 78: 359-368

Walsh EG (1976) Clonus: beats provoked by the application of a rhythmic force. J Neurol Neurosur Ps 39: 266-274

Winter DA, Patla AE (1997) Signal processing and linear systems for the movement sciences. Waterloo Biomechanics, Waterloo, Ontario

Young RR (1984) Physiological and enhanced physiological tremor. In: Findley LJ, Capildeo R (eds) Movement disorders: Tremor. Macmillan, London, pp 127-134

Young RR, Hagbarth KE (1980) Physiological tremor enhanced by manoeuvres affecting the segmental stretch reflex. J Neurol Neurosur Ps 43: 248-256

Zahalak GI, Cannon SC (1983) Predictions of the existence, frequency, and amplitude of physiological tremor in normal man based on measured frequency-response characteristics. J Biomech Eng 105: 249-257

Zahalak GI, Heyman SJ (1979) A quantitative evaluation of the frequency-response characteristics of active human skeletal muscle in vivo. Trans ASME 101: 28-37

Figure Legends

Figure 1: a) The power spectrum and b) a three second sample of the 4.5 Hz narrow band stimulus with a mean rectified displacement of 1.3^{o}.

Figure 2: Samples of the position signal (upper trace of each pair) and EMG (lower trace of each pair) for one subject at the same mean rectified stretching amplitude of 1.9^{o} but at two different frequencies: a) 0.5 Hz and b) 8.5 Hz.

Figure 3: Mean amplitude spectra of the IEMG for all subjects using the different narrow band stretching stimuli. The centre frequencies of the stretching stimuli are indicated by the sloping dashed lines. The spectra for each subject have first been normalised to the maximum amplitude across all conditions. The mean for all subjects within each condition was then calculated. Each mean spectrum has then been scaled to the maximum for display purposes.

Figure 4: Mean across all subjects of the fraction of the total power to 25 Hz of the IEMG in a band from 10.5 - 15 Hz ('Tremor') and in a 2 Hz band centred about the stretching frequency ('Stretch') shown at the five different stretching amplitudes and 10 stretching frequencies.

Figure 5: IEMG power spectra for one subject with five different stimulus amplitudes and 10 different centre frequencies. The centre frequencies are indicated by the sloping dashed lines. In order to provide a finer frequency resolution of 0.05 Hz for this figure only, the rectified EMG signals were low pass

filtered (20 Hz cut-off, 6^{th} order Butterworth), resampled at 100 Hz and then a fast Fourier transform was computed and squared. Note that in contrast with Figure 3, all spectra are shown here on the same scale of absolute EMG power.

Figure 6: The mean across all subjects of the overall coherence between the wrist angle and the IEMG as a function of each amplitude and frequency of stretch.

Figure 7: Output from the simple open-loop reflex model consisting of a spindle as a front end for a simple integrate-and-fire neuron. a) A constant input is used to the neuron providing a background firing rate of 12 Hz. b), c) and d) Sinusoidal inputs having the frequencies and relative amplitudes shown are input to the spindle model, superimposed on the 12 Hz background firing of the neuron.

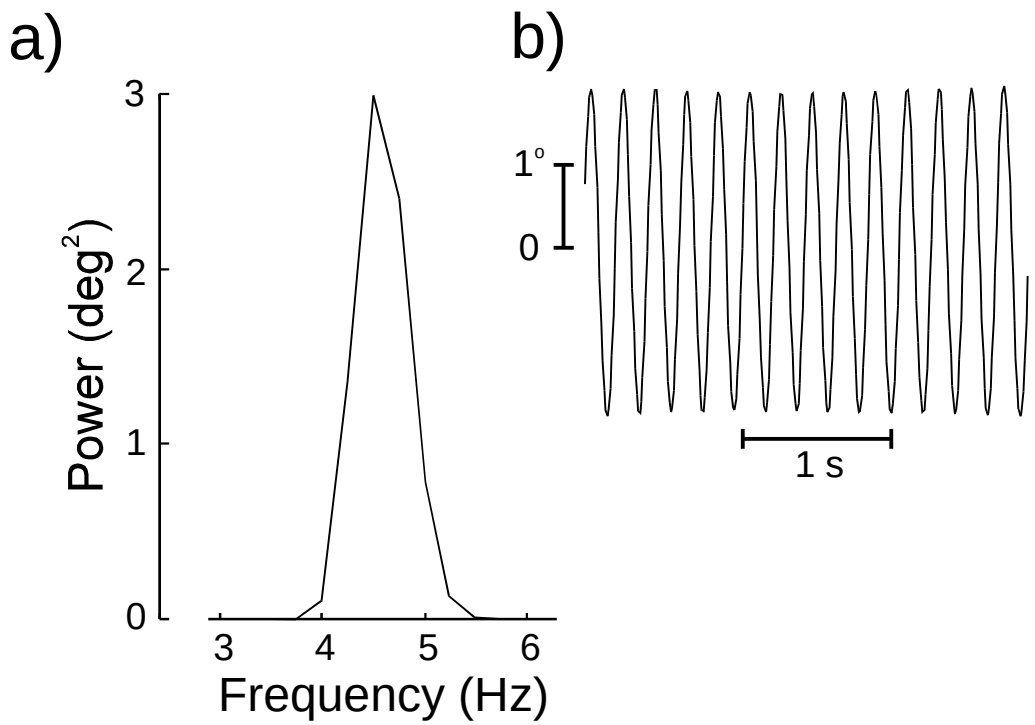

Fig 1

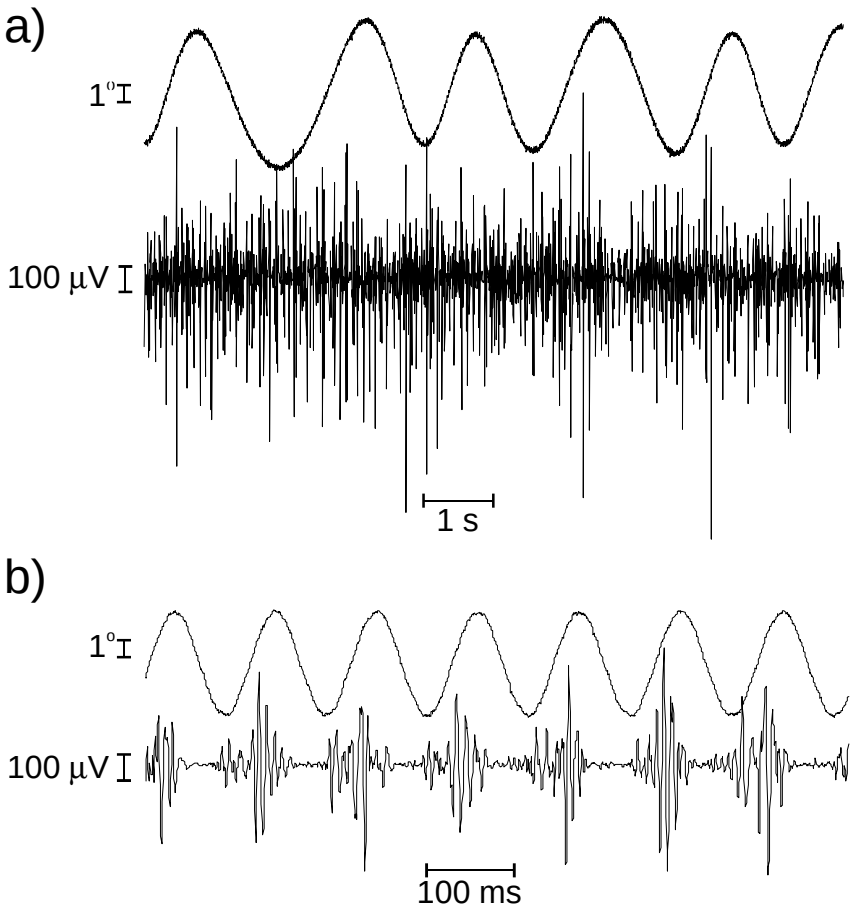

Fig 2

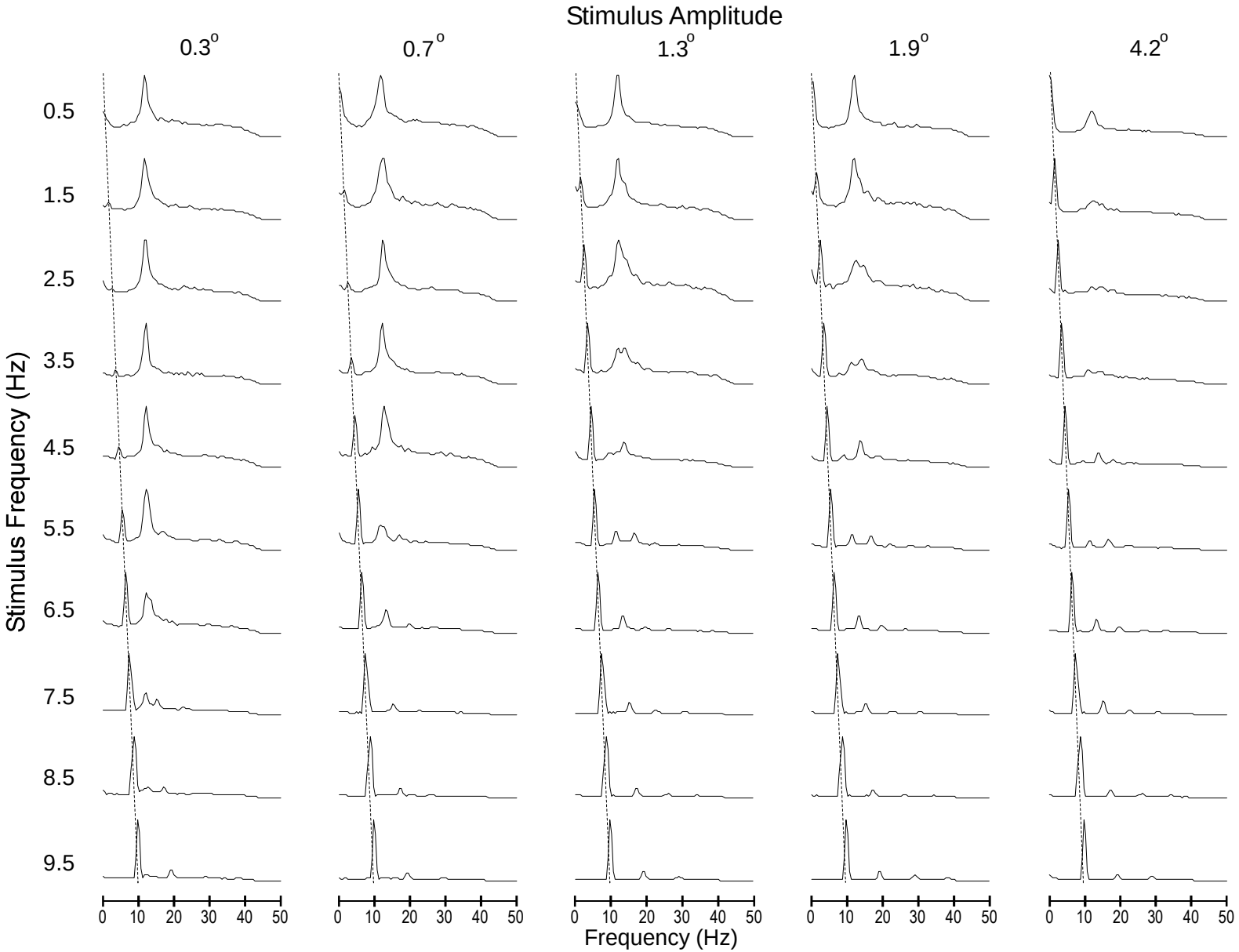
Stimulus Amplitude
0.3°
0.7°
1.3°
1.9°
4.2°
Stimulus Frequency (Hz)
0.5
1.5
2.5
3.5
4.5
5.5
6.5
7.5
8.5
9.5
0 10 20 30 40 50
Frequency (Hz)

Fig 3

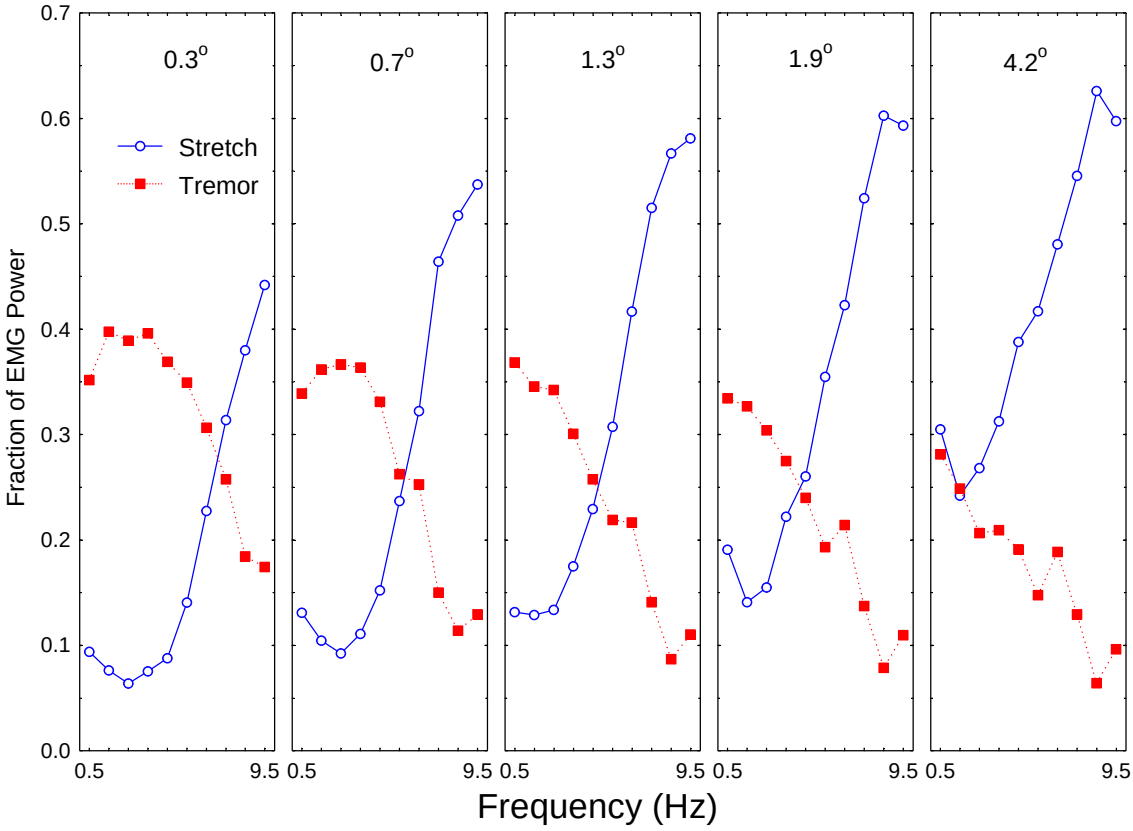
0.3°
0.7°
1.3°
1.9°
4.2°
Stretch
Tremor
Fraction of EMG Power
0.0
0.1
0.2
0.3
0.4
0.5
0.6
0.7
0.5
9.5
Frequency (Hz)

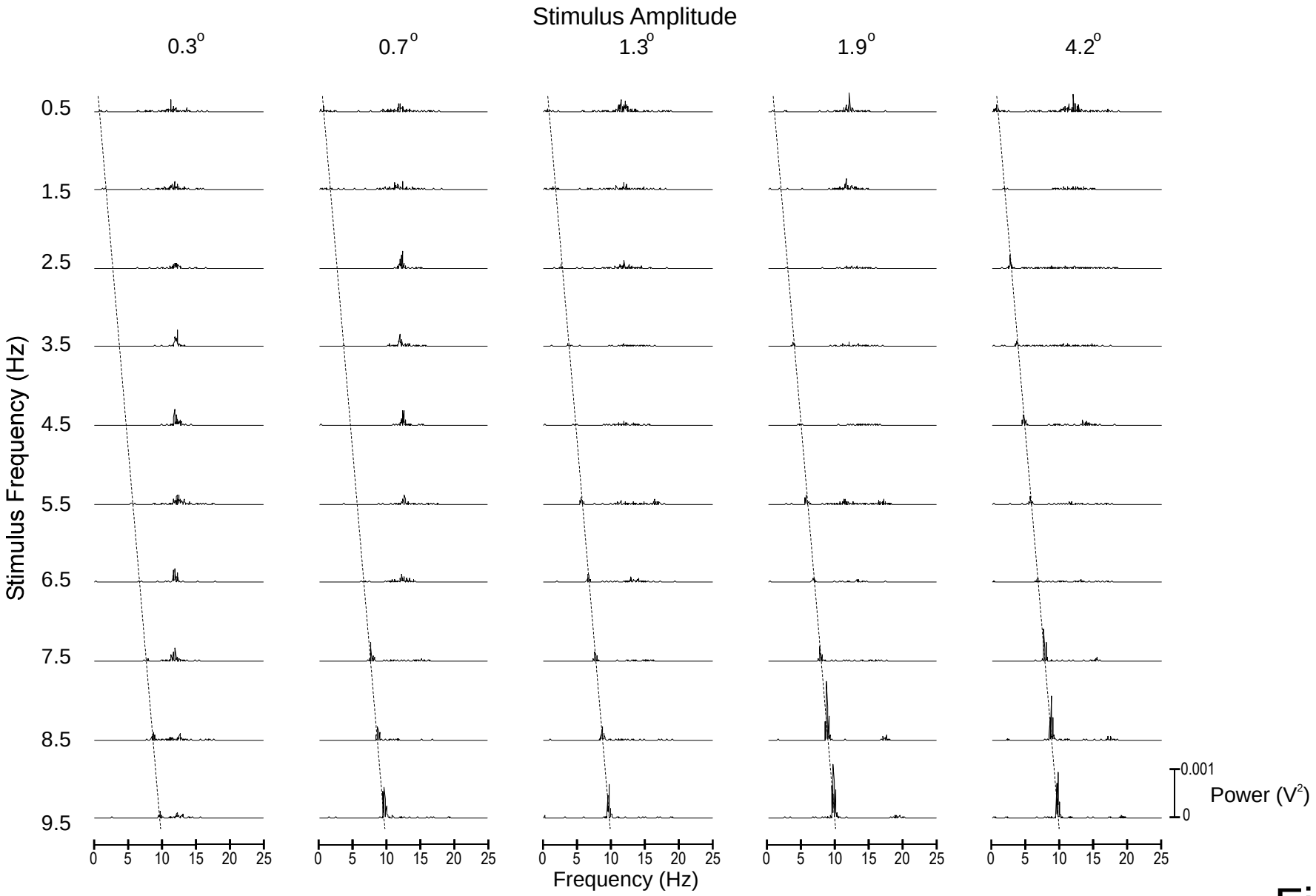
Stimulus Amplitude
0.3°
0.7°
1.3°
1.9°
4.2°
Stimulus Frequency (Hz)
0.5
1.5
2.5
3.5
4.5
5.5
6.5
7.5
8.5
9.5
0 5 10 15 20 25
Frequency (Hz)
0.001
0
Power (V²)

Fig 5

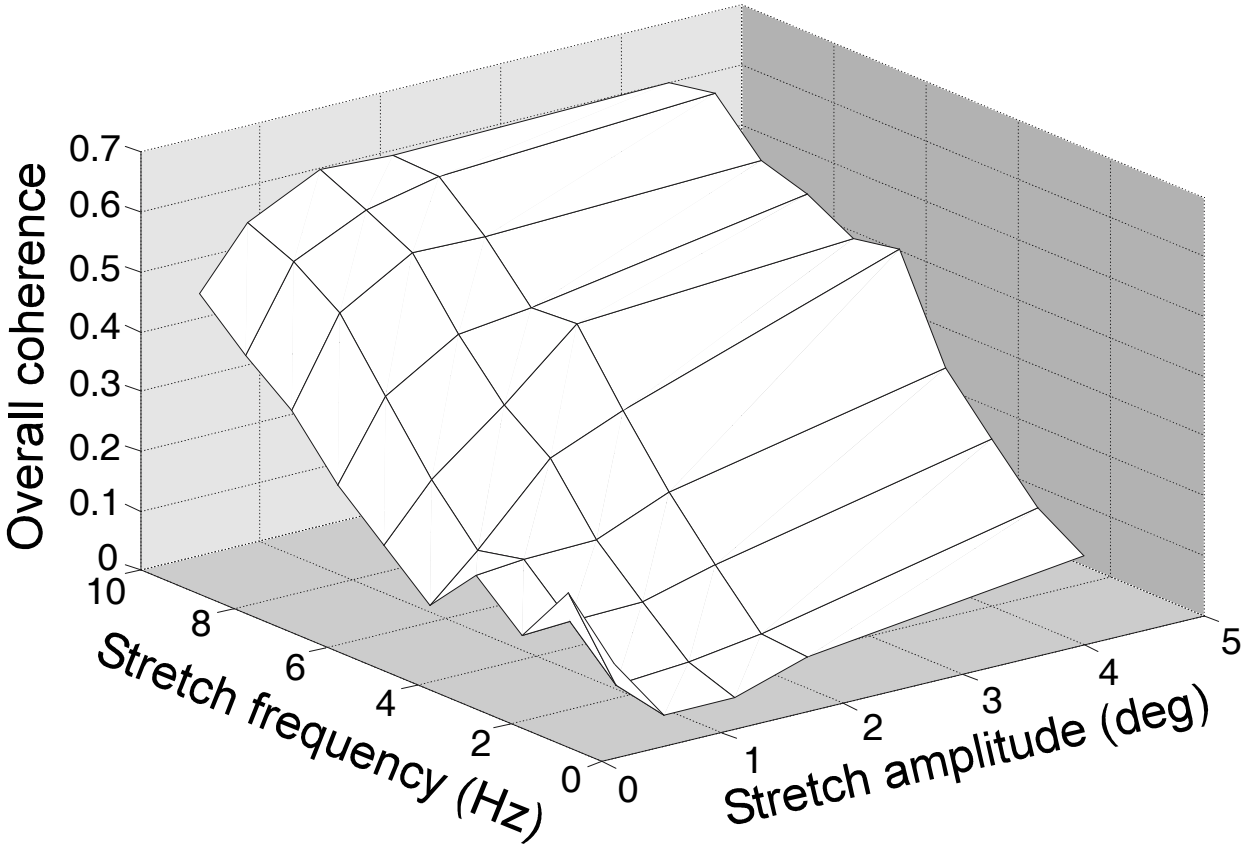
Overall coherence
0.7
0.6
0.5
0.4
0.3
0.2
0.1
0
10
8
6
4
2
0
Stretch frequency (Hz)
0
1
2
3
4
5
Stretch amplitude (deg)

Fig 6

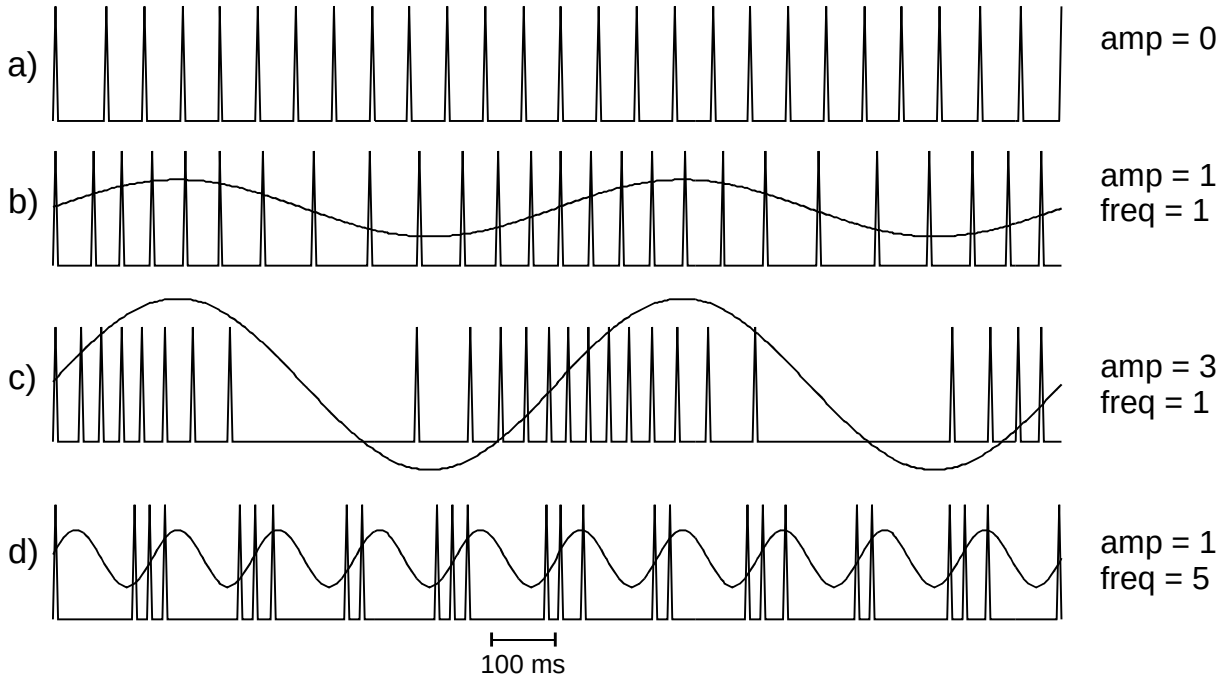

Fig 7